

# Characteristics of an Ion Beam in a Magnetically Expanding Plasma using Permanent Magnets

Kazunori TAKAHASHI<sup>\*1</sup> and Tamiya FUJIWARA<sup>\*1</sup>

## Abstract

Generation of a supersonic ion beam is observed in a low-pressure solenoid-free plasma expanded by permanent magnet arrays. By employing double concentric arrays of permanent magnets, a constant field area of about 100 G in a source tube, and a diverging magnetic field near the exit of the plasma source can be generated, where the source consists of a 6.5-cm-diameter glass tube and a double-turn rf loop antenna. The 13.56 MHz rf power is maintained at 250 W and the operating argon gas pressure can be changed from about 0.3 – 2.5 mTorr. Ion energy distribution function is measured by a combination of a retarding field energy analyzer and a pulsed probe technique. As a result, it is found that the beam energy can be increased up to about 40 eV with a decrease in the operating gas pressure.

**Keywords:** Magnetically expanding plasma, Double layer, Ion beam, Permanent magnets, Electric propulsion device

## 1. Introduction

Plasma expansions have attracted a great deal of attention because it self-consistently forms nonlinear plasma-potential structures causing electrostatic particle acceleration and deceleration. The process has been investigated in laboratory plasmas in connection with space plasmas<sup>[1]</sup> and electric propulsion devices<sup>[2]</sup>. Since the formation of the current-free double layer (DL) and the subsequent ion acceleration in a magnetically expanding plasma were reported<sup>[3,4]</sup>, much attention is recently focused on this kind of research in the electric propulsion community because it would lead to the new type of electric thruster, named the helicon double layer thruster<sup>[5-8]</sup>, without any electrode for plasma productions and ion accelerations. In general, this kind of thruster requires the electromagnets for the production of the expanding magnetic-field configuration, which consume much electricity, and make the system large and costly. From the viewpoint of the practical use to the electric thruster, it is important to reduce the consumed electricity and the weight. In order to reduce the power consumption and weight in the system, authors have suggested the new type of the magnetically expanding plasma using only permanent magnets for the generation of the ion beam, which has briefly reported in the previous papers<sup>[7,8]</sup>. In this experiment, the rapid potential drop with about 3-4 cm thickness is generated near the exit of the plasma source. It is very important to know the detailed characteristics of the ion beams generated by the DL, especially effects of the external parameters such as the gas pressure, magnetic-field configuration, rf power, and so on, for practical use to the thruster.

In the present paper, we report the ion beam behavior in the solenoid-free expanding argon plasmas using only permanent magnets, when the operating gas pressure is changed. The ion energy distribution functions are measured by a retarding field energy analyzer (RFEA), where the I-V curve of the analyzer is differentiated through the active analogue circuit. As a result of the accurate measurements, it is found the ion beam energy can be increased up to about 40 eV with a decrease in the operating argon gas pressure.

---

\* 1 Department of Electrical and Electronic Engineering, Iwate University

## 2. Experimental setup

### 2.1. Magnet configuration

The magnetic fields produced by the permanent magnets are strongly nonuniform with reverse-fields, i.e., cusps. According to the previous experiments performed by Shamrai *et al.*<sup>[9]</sup>, the cusp fields prevent the plasma diffusion, the DL formation, and the ion beam generation in the plasmas. Thus, it is required that the magnetic-field configuration has a constant-field area around the plasma production region, and the diverging-field area without any cusp fields. In order to provide the above-mentioned constant-field and diverging-field areas, double concentric arrays of the permanent magnets as shown in Fig. 1(a) are set around the plasmas source, where each arrays consists of eight Neodymium Iron Boron (NdFeB) magnets (10 cm in length, 1.5 cm in width, and 0.5 cm in thickness). All of the magnets have inward magnetization in the radial direction, i.e., in the direction of thickness. The top and bottom of Fig. 1(b) shows the images of the magnetic-field lines produced by the single and double concentric arrays of the permanent magnets. As shown in the top of Fig. 1(b), the single array of the magnets can produce the diverging magnetic fields, while the cusp fields exist at the axial center of the magnet bars. Between the cusp and the diverging fields, there is no constant field area for the case of the single magnet arrays. On the other hand, the double magnet arrays can create both the constant field area and the diverging fields without the cusp at the radial center. By employing this double magnet arrays around the source tube, the expanding magnetic-field configuration can be created near the source exit. The observed and calculated magnetic field strengths are described in the next section.

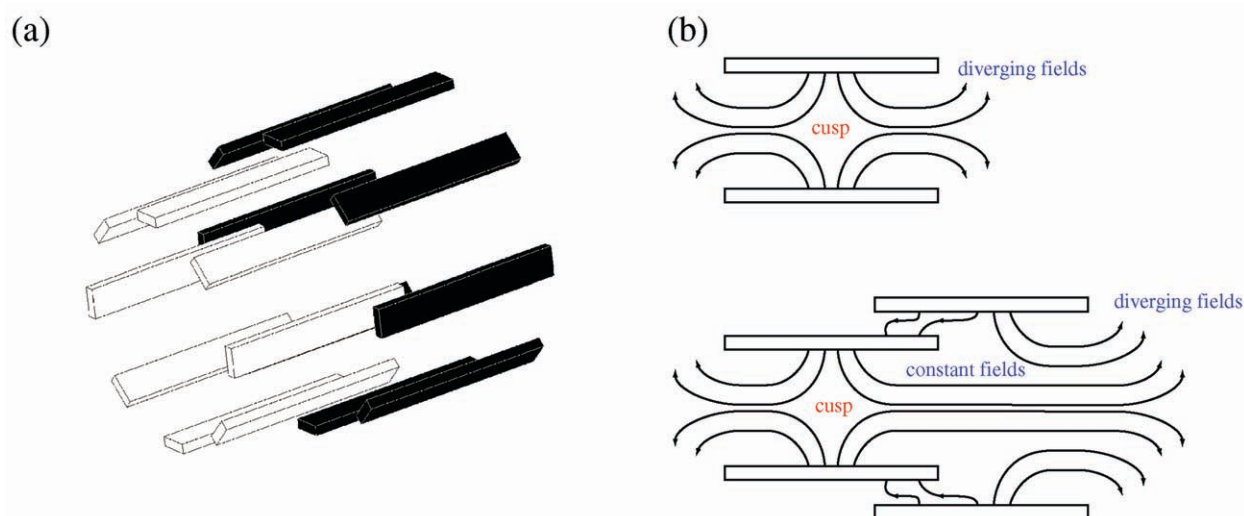


Fig.1 (a) Configuration of the permanent magnets. (b) Images of the magnetic-field lines created by the single magnet array (top) and the double magnet arrays (bottom).

### 2.2. Machine configuration

A schematic diagram of the experimental setup is shown in Fig. 2(a) and has already reported by authors<sup>[7]</sup>. Briefly, a cylindrical glass tube of 20 cm in length and 6.5 cm in inner diameter (source tube) is attached contiguously to a 26-cm-diameter and 30-cm-long grounded stainless steel vacuum chamber (diffusion chamber). The chamber is evacuated to a base pressure of  $2 \times 10^{-6}$  Torr by a  $700 \text{ ls}^{-1}$  diffusion/rotary pumping system, and the argon gas is introduced from the source side through a mass flow controller. The argon gas pressure in the vacuum chamber can be maintained in the range of 0.1 – 3 mTorr. An argon plasma is excited by a 7.5-cm-diameter two-turn loop antenna located at  $z = -9$  cm and powered from an rf generator of frequency 13.56 MHz and power 250 W, where  $z = 0$  is defined as the exit of the glass source tube. Surrounding the source tube and the rf antenna, the double concentric arrays of the permanent magnets described in the previous section are arranged for generation of the expanding magnetic-field configuration as shown in Fig. 2(a). The calculated and experimentally measured axial component of the local magnetic-field strengths are presented in Fig. 2(b) as solid line and closed circles, respectively, where the data are from Ref.<sup>[7]</sup>. The calculated field strength is fairly in agreement with the experimentally measured one. It is found that there is no cusp, i.e., null point of  $B_z$ , near the plasma production area ( $z = -9$  cm) and diverging field area, although the cusp is formed in the upstream side ( $z \sim -16$  cm) of the source. The insulator plate is inserted in front of the upstream flange

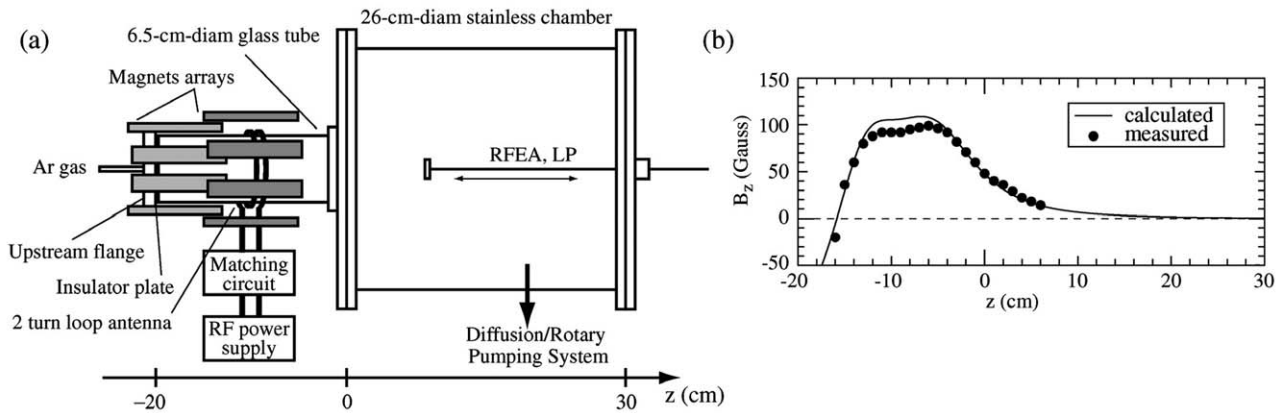


Fig. 2 (a) Schematic diagram of experimental setup. (b) Axial profile of the calculated (solid line) and experimentally observed (closed circle) axial component  $B_z$  of the magnetic-field strength produced by the double concentric permanent magnets arrays.

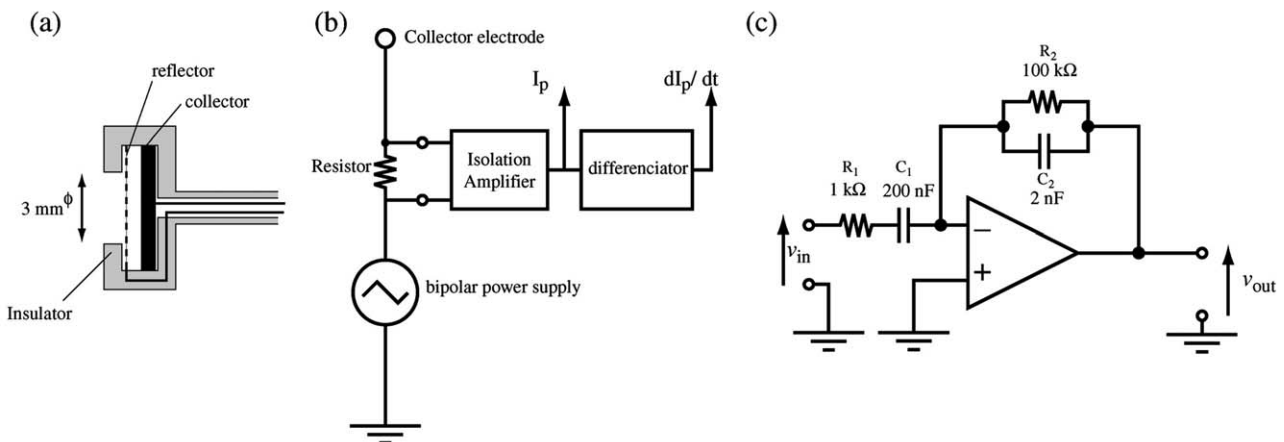


Fig. 3 (a) Schematic diagram of the retarding field energy analyzer (RFEA). (b) Measurement circuit of the ion energy distribution function (IEDF:  $-dI_c / dV_c$ ). (c) Circuit diagram of the differentiator.

for making the condition of the “current free”, which means the net current in the axial direction of the system is equal to zero. Under these conditions, we have already reported that the rapid potential drop of the DL is spontaneously generated near the source exit ( $z \sim -2 - 1$  cm) and the ion beam accelerated by the DL structure is detected in the diffusion chamber downstream of the DL [7].

### 2.3. Ion diagnosis

The ion energy distribution functions (IEDFs) in the axial direction are measured by a retarding field energy analyzer (RFEA) located at  $z = 3$  cm downstream of the DL. The schematic diagram of the RFEA is shown in Fig. 3(a), which consists of an electron reflector mesh biased at  $-60$  V, an ion collector electrode, and a 3-mm-diameter entrance orifice, where the IEDF is obtained as the first derivative curve of the  $I_c - V_c$  characteristic, where  $I_c$  and  $V_c$  are the current and voltages of the collector electrode. When the collector bias voltage is set at 100 V, it is confirmed that the collector current is almost zero. Hence, we can deduce the effects of the secondary electrons are very little. Estimation of the derivative curve from the  $I - V$  curve is difficult because of the digital noise. When the voltage  $V_c$  is linearly swept ( $dV_c/dt = \text{constant}$ ) and  $I_c$  is in a steady state,  $dI_c/dt$  is proportional to the first derivative of  $I_c - V_c$  curve. Therefore, the IEDF can be directly obtained by measurement of the first derivative of  $I_c - t$  characteristic when  $V_c$  is swept linearly. Figure 3(b) shows the measurement circuit of the IEDF, which is called “pulsed probe technique” [10]. Outside the plasma the current signal is passed through a resistor and then is connected to a bipolar power voltage source that is swept for 25 msec from  $+120$  V to  $-20$  V. The voltage signal from the resistor is fed through an isolation amplifier to an active analog circuit in Fig. 3(c). The voltage gain  $G_v$  ( $\equiv v_{\text{out}} / v_{\text{in}}$ ) of the active analog circuit in Fig. 3(c) can be derived as

$$G_v = -\frac{R_1}{R_2} \frac{1}{\left(1 + \frac{1}{j\omega C_1 R_1}\right)(1 + j\omega C_2 R_2)} = -\frac{R_1}{R_2} \frac{1}{\left(1 + \frac{1}{j\omega T}\right)(1 + j\omega T)}, \quad (1)$$

where  $T$  is defined as  $T \equiv R_1 C_1 = R_2 C_2$  for simplification. In this experiment, the circuit parameters are set as  $R_1 = 1 \text{ k}\Omega$ ,  $C_1 = 200 \text{ nF}$ ,  $R_2 = 100 \text{ k}\Omega$ , and  $C_2 = 2 \text{ nF}$ , respectively. For low ( $\omega T \ll 1$ ) and high ( $\omega T \gg 1$ ) frequency conditions, the gain can be simplified as  $G_v = -j\omega C_1 R_2$  (differentiator), and  $G_v = -1/(j\omega) C_2 R_1$  (integrator), respectively. Hence, the active circuit acts both as differentiators for the current signal during slow voltage sweep and as rejecting filters for plasma instabilities and electric noises above  $1 \text{ kHz}$  [10]. Finally, the differentiated signal are digitized by a digital storage oscilloscope (Tektronix TDS 2024 B), and passed into a LABVIEW program for converted into an ASCII data file and display on a computer.

### 3. Experimental results

Figure 4(a) shows the collector bias voltage (dotted line), the normalized ion current signal of the RFEA (dotted-dashed line), and the normalized first derivative (solid line) of the ion current as a function of time for the gas pressure  $P_{Ar} = 0.35 \text{ mTorr}$ , where the RFEA is set at  $z = 3 \text{ cm}$  downstream of the DL and the data are the average over many shots. It is found that the first derivative characteristic can precisely be obtained by the above-mentioned pulsed probe technique.

From the results in Fig. 4(a) we can obtain the IEDF as shown in Fig. 4(b). The IEDF in Fig. 4(b) clearly shows the two peaks around the collector bias voltages of  $V_c \sim 30 \text{ V}$  and  $65 \text{ V}$ , where the low-energy side peak shows the bulk ions and the  $V_c$  yielding this peak shows the local plasma potential  $\phi_p$  indicated as arrow in Fig. 4(b). Here, the IEDF appears to be broadened due to the effects of the radio-frequency electric field [4], but we can estimate the ion beam energy. In order to analyze the observed IEDF, three Gaussian deconvolutions are plotted together with the observed IEDF as the dotted, dashed, and dotted-dashed lines in Fig. 4(b). The highest-energy component around  $V_c \sim 65 \text{ V}$  shows the accelerated group of ions, i.e., the ion beam. We define  $V_c$  yielding the high-energy peak as a beam potential  $\phi_{\text{beam}}$ . Note that the ‘‘beam potential’’ is different from the ‘‘beam energy’’. According to the principle of the RFEA measurements, zero energy corresponding to the local plasma potential  $\phi_p$ . Therefore, the ‘‘ion beam energy’’  $\varepsilon_{\text{beam}}$  can be estimated as  $\varepsilon_{\text{beam}} = \phi_{\text{beam}} - \phi_p$ ; the energy of the ion beam observed in Fig. 4(b) is identified as  $\varepsilon_{\text{beam}} \sim 35 \text{ eV}$ . As reported in previous works [7], the beam energy is in good agreement with the potential drop  $\phi_{\text{DL}}$  of the DL near the source exit. Therefore, the ions created in the upstream rf plasma source are

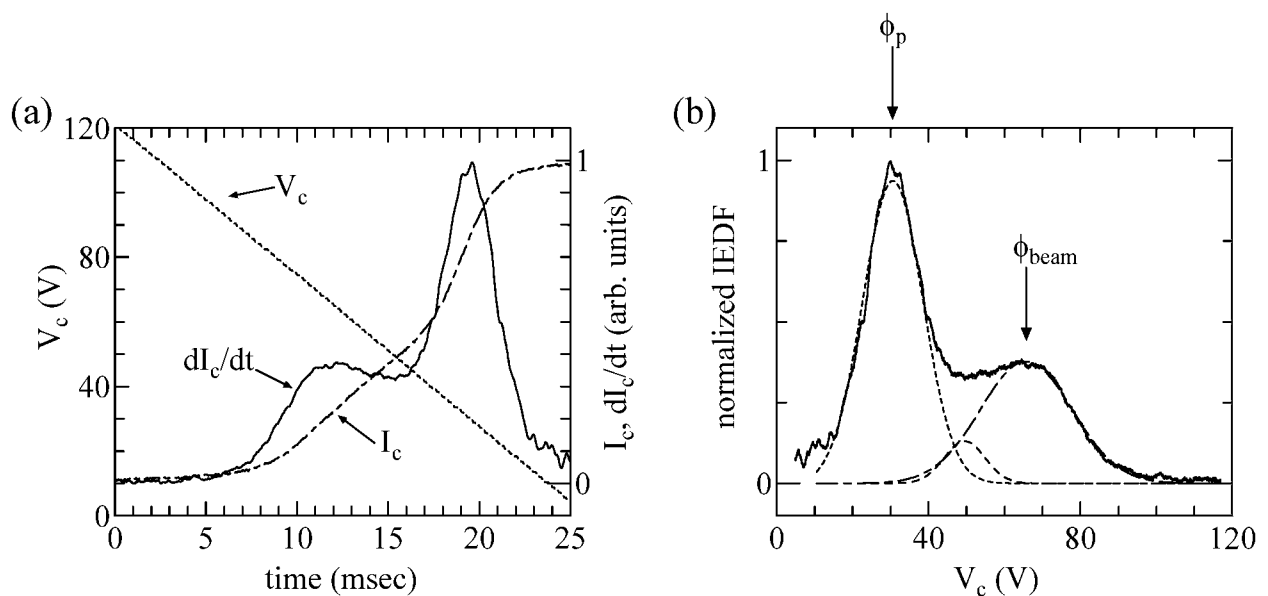


Fig. 4 (a) Collector bias voltage (dotted line), ion current of the RFEA (dotted-dashed line), and the first derivative (solid line) of the ion current as a function of time for  $P_{Ar} = 0.35 \text{ mTorr}$ , where the RFEA is set at  $z = 3 \text{ cm}$  downstream of the DL. (b) Normalized ion energy distribution function (IEDF) obtained from Fig. 4(a) together with three Gaussian deconvolutions (dotted, dashed, and dotted-dashed lines).

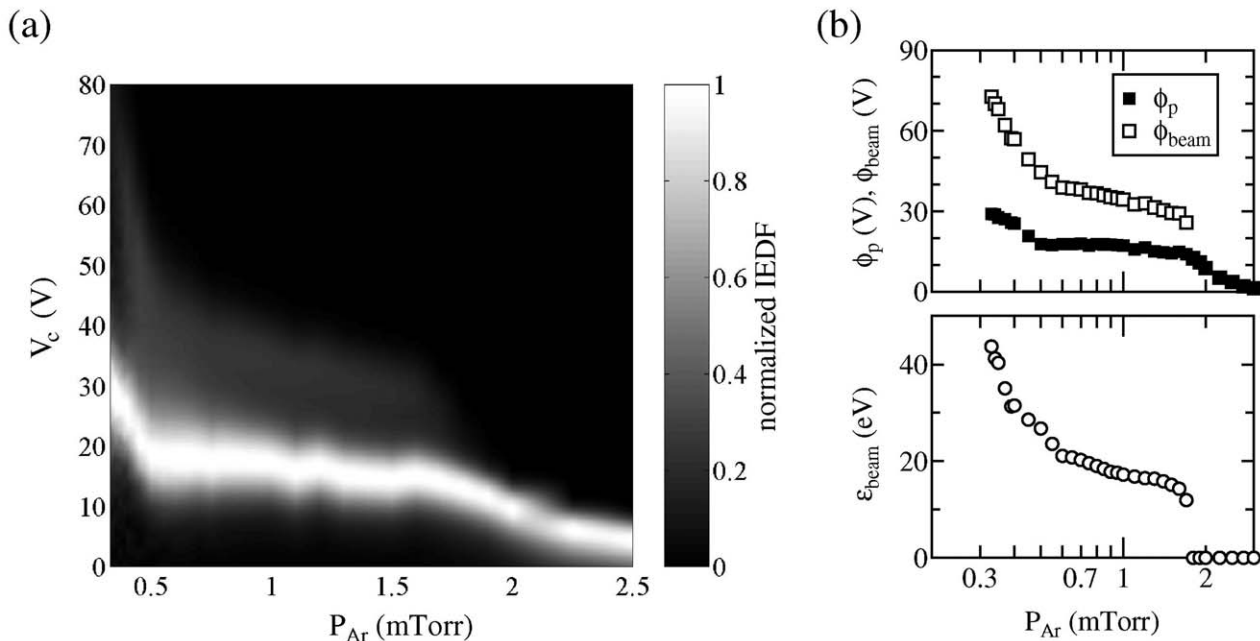


Fig. 5 (a) Ion energy distribution functions (IEDFs) normalized by the maximum of the IEDF at each gas pressure, as a function of the operating argon gas pressure  $P_{\text{Ar}}$  at  $z = 3$  cm. (b) The local plasma potential  $\phi_p$  (closed squares), the beam potential  $\phi_{\text{beam}}$  (open squares), and the ion beam energy  $\epsilon_{\text{beam}}$  (open circles) obtained from the IEDFs shown in Fig. 5(a) as a function of the gas pressure  $P_{\text{Ar}}$ .

accelerated by the DL potential drop. Here, we need to mention another peak in the Gaussian deconvolutions around  $V_c \sim 50$  V. Although the detail is unclear now, we expect that the peak around  $V_c \sim 50$  V is due to elastic collisions with neutral particles.

The ion beam velocity  $v_{\text{beam}}$  can be derived as

$$v_{\text{beam}} = \sqrt{\frac{2e\epsilon_{\text{beam}}}{M_i}}, \quad (2)$$

where  $M_i$  is the mass of the argon ion. Under the present operating conditions, the beam velocity of ions with  $\epsilon_{\text{beam}} \sim 35$  eV can be estimated as  $v_{\text{beam}} \sim 13$  km/sec. The electron temperature obtained from the rf uncompensated Langmuir probe is  $T_e \sim 8$  eV. The ion sound speed is  $C_s \sim 4.4$  km/sec for the electron temperature  $T_e \sim 8$  eV. Therefore, the Mach number  $M$  of the ion beam is estimated as  $M \sim 3$  and is found to be supersonic.

Figure 5(a) shows the normalized IEDFs as a function of the gas pressure  $P_{\text{Ar}}$ , observed at  $z = 3$  cm, where the IEDFs are obtained at discrete gas pressure and normalized by the maximum for each gas pressure. As shown in Fig. 5(a), the energetic or beam ions are detected below the pressure of about 2 mTorr. The local plasma potential  $\phi_p$ , the beam potential  $\phi_{\text{beam}}$ , and the ion beam energy  $\epsilon_{\text{beam}}$  are obtained from the IEDFs shown in Fig. 5(a), and plotted in Fig. 5(b) as closed squares, open squares, and open circles, respectively. It is found that the ion beam energy  $\epsilon_{\text{beam}}$  is strongly depending on the operating gas pressure and decreases with an increase in the gas pressure  $P_{\text{Ar}}$ . In addition, the ion beam disappears at around 2 mTorr. Around the pressure of 2 mTorr, the mean free path of the electron – neutral collisions are very close to the machine length, although the detailed physics are unclear under the present stage. The observed behavior of the ion beam in this experiment resembles the theoretically predicted and experimentally observed ones in the magnetically expanding plasmas using electromagnets<sup>[11-13]</sup>. But, this experiment shows the first result on the generation of the supersonic ion beam in the magnetically expanding “solenoid-free” plasma using only permanent magnets, which would yield the high efficiency of the total system of the ion engine by eliminating the electromagnets and its power supply.

#### 4. Conclusion

The characteristics of the ion beam generated by the double layer (DL) in the magnetically expanding plasma using permanent magnets are experimentally investigated by the retarding field energy analyzer (RFEA) located at the downstream side of the DL. The ion energy distribution functions (IEDFs) are measured by the retarding field energy analyzer, where the first derivative of the I-V curve is precisely obtained by the pulsed probe technique using analog differentiator. The observed IEDFs evidences the generation of the ion beam due to the spontaneous formation of the DL near the source exit. The beam energy can be increased up to about 40 eV with a decrease in the operating argon gas pressure. The typical Mach number  $M$  of the ion beam is estimated from the RFEA measurements and the Langmuir probe measurements as  $M \sim 3$  and the beam is found to be supersonic.

#### Acknowledgements

The authors are indebted to Y. Shida for his technical assistance. This work was partially supported by Grant-in-Aid for Young Scientists (Grant No. 20740317) from the Ministry of Education, Culture, Sports, Science and Technology, Japan. This work is also partially supported by TEPCO Research Foundation, Yazaki Memorial Foundation for Science and Technology, and the Foundation for the Promotion of Ion Engineering.

#### References

- [1] G. Hairapetian and R. L. Stenzel, "Expansion of a two-electron-population plasma into vacuum", *Physical Review Letters*, vol. 61, p. 1607, 1988.
- [2] S. A. Cohen, N. S. Siefert, S. Stange, R. F. Boivin, E. E. Scime, and F. M. Levinton, "Ion acceleration in plasmas emerging from a helicon-heated magnetic-mirror device", *Physics of Plasmas*, vol. 10, p. 2593, 2003.
- [3] C. Charles and R. W. Boswell, "Current-free double-layer formation in a high-density helicon discharge", *Applied Physics Letters*, vol. 82, p. 1356, 2003.
- [4] C. Charles and R. W. Boswell, "Laboratory evidence of a supersonic ion beam generated by a current-free helicon double-layer", *Physics of Plasmas*, vol. 11, p. 1706, 2004.
- [5] C. Charles and R. W. Boswell, "The magnetic-field-induced transition from an expanding plasma to a double layer containing expanding plasma", *Applied Physics Letters*, vol. 91, p. 201505, 2007.
- [6] M. D. West, C. Charles, and R. W. Boswell, "Testing a helicon double layer thruster immersed in a space-simulation chamber", *Journal of Propulsion and Power*, vol. 24, p. 134, 2008.
- [7] K. Takahashi, K. Oguni, H. Yamada, and T. Fujiwara, "Ion acceleration in a solenoid-free plasma expanded by permanent magnets", *Physics of Plasmas*, vol. 15, p. 084501, 2008.
- [8] K. Takahashi and T. Fujiwara, "Observation of weakly and strongly diverging ion beams in a magnetically expanding plasma", *Applied Physics Letters*, vol. 94, p. 061502, 2009.
- [9] K. P. Shamrai, Y. V. Virko, V. F. Virko, and A. I. Yakimenko, "Compact helicon plasma source with permanent magnets for electric propulsion application", *Proceedings of the 42nd AIAA/ASME/SAE/ASEE Joint Propulsion Conference and Exhibit, California*, (AIAA, New York, 2006) p. 4845, 2006.
- [10] K. Takahashi, C. Charles, R. W. Boswell, T. Kaneko, and R. Hatakeyama, "Measurement of the energy distribution of trapped and free electrons in a current-free double layer", *Physics of Plasmas*, vol. 14, p. 114503, 2007.
- [11] M. A. Lieberman and C. Charles, "Theory for formation of a low-pressure, current-free double layer", *Physical Review Letters*, vol. 97, p. 045003, 2006.
- [12] M. A. Lieberman, C. Charles, and R. W. Boswell, "A theory for formation of a low pressure, current-free double layer", *Journal of Physics D*, vol. 39, p. 3294, 2006.
- [13] O. Sutherland, C. Charles, N. Plihon, and R. W. Boswell, "Experimental evidence of a double layer in a large volume helicon reactor", *Physical Review Letters*, vol. 95, p. 205002, 2005.